Gut microbiota associated with obesity and high carotid intima-media thickness among Chinese children

Jiahong Sun
Shandong University
Xuli Jin
Shandong University
Liu Yang
Shandong University
Xiaoyun Ma
Shandong University
Bo Xi
Shandong University https://orcid.org/0000-0003-0491-5585
Suhang Song
University of Georgia https://orcid.org/0000-0003-1934-632X
Min Zhao (zhaomin1986zm@126.com)
Shandong University

Article

Keywords: gut microbiota, cardiovascular disease, obese, cIMT, children

Posted Date: June 16th, 2022

DOI: https://doi.org/10.21203/rs.3.rs-1622498/v1

Abstract

Background

High carotid intima-media thickness (cIMT) in childhood, usually combined with obesity, is an early predictor of cardiovascular disease (CVD) later in life. However, the association between gut microbiota and high cIMT among children with obesity remains unclear. Therefore, we compared differences in composition, community diversity, and richness of gut microbiota among children with obesity and high cIMT (OB + high-cIMT), obesity but normal cIMT (OB + non-cIMT), and normal weight and normal cIMT (i.e., normal children) to identify differential microbiota biomarkers.

Methods

A total of 24 OB + high-cIMT children, 24 OB + non-cIMT children, and 24 normal children aged 10–11 years from the Huantai Childhood Cardiovascular Health Cohort Study were included. All included fecal samples were tested using 16S rRNA sequencing. *α*-diversity analysis was performed to estimate the community richness and diversity of gut microbes, and LEfSe analysis was used to reveal the main differential biomarkers among these three groups. Random forest analysis was used to further select differential biomarkers. The receiver operating characteristic (ROC) curve was used to evaluate the ability of biomarkers in identifying OB + non-cIMT and OB + high-cIMT. Kyoto Encyclopedia of Genes and Genomes (KEGG) pathways were assessed by Phylogenetic Investigation of Communities by Reconstruction of Unobserved States (PICRUSt) according to the KEGG database.

Results

The community richness and diversity of gut microbiota in OB + high-cIMT children were decreased compared with OB + non-cIMT children and normal children. At the genus level, the relative abundances of *Christensenellaceae_R-7_group*, *UBA1819*, *Family_XIII_AD3011_group*, and *unclassified_o__Bacteroidales* were reduced in OB + high-cIMT children compared with OB + non-cIMT and normal children. In addition, these four significant biomarkers were ranked in the top 1, 2, 6, and 12 in the random forest analysis. ROC analysis results showed that combined *Christensenellaceae_R-7_group*, *UBA1819*, *Family_XIII_AD3011_group*, and *unclassified_o__Bacteroidales* performed high ability in identifying OB + high-cIMT (area under the curve [AUC]: 0.91, 95% CI = 0.82–1.00]) and moderate ability in identifying OB + non-cIMT (AUC 0.76, 95% CI = 0.62–0.91). PICRUSt showed unique thiamine metabolism and methane metabolism pathways in gut microbial were decreased in OB + high-cIMT compared with OB + non-cIMT.

Conclusion

Gut microbiota plays a pivotal role in detecting children with obesity combined with high cIMT.

Introduction

Cardiovascular disease (CVD) is a major public health issue, which may result in a decline in life expectancy, and an increase in economic burden and the risks of premature deaths (1–3). High carotid intima-media thickness (cIMT) was determined by the guidelines of the American College of Cardiology Foundation/American Heart Association as a class IIa recommendation for intermediate-risk assessment of asymptomatic CVD (4). A recent meta-analysis of 119 clinical trials showed that reduction in the degree of CVD can be predicted by the intervention on the progress of high cIMT (5). The measurement of cIMT is essential in adults with obesity, which is a main modifiable risk factor of CVD later in life (6). Emerging evidence shows that cIMT was used as one of the promising parameters to measure whether obese patients are qualified for bariatric surgery (7–9). We have previously found that the combination of general obesity and abdominal obesity was strongly associated with high cIMT among children (10). Therefore, early detection of obesity and high cIMT among children is of great significance to track the progress of obesity among children, which can provide guidance for early prevention of CVD in later life.

The gut microbiota has been considered to be a very promising target for the prevention and treatment of CVD in adults (11–13). A large number of clinical and experimental studies have shown that gut microbes play a key role in the occurrence and development of obesity mainly by regulating host energy metabolism, substrate metabolism, and inflammatory pathophysiological mechanisms in adults and children (14–19). However, little is known about the specific gut microbiota associated with the progress of obesity (i.e., obesity and high cIMT [OB + high-cIMT]) in children.

Therefore, in this study, we aimed to compare the composition, relative abundance, and community diversity of the gut microbiota among children with OB + high-cIMT, children with obesity but normal cIMT (OB + non-cIMT), and children with normal weight and normal cIMT, and revealed main gut microbiota biomarkers using 16S rRNA sequencing.

Methods

Study population

Data were collected from the Huantai Childhood Cardiovascular Health Cohort Study at baseline conducted in a public elementary school in Huantai County, Zibo City, Shandong Province, China, between November 2017 and January 2018. In the current study, 24 children aged 10–11 years with obesity and high cIMT, 24 children with obesity but normal cIMT, and 24 children with normal weight and normal cIMT matched by age and sex were included. This study was approved by the Ethics Committee of the School of Public Health of Shandong University (approval number: 20160308), and written informed consent was obtained from all the investigated children and their parents or guardians (20).

Anthropometric measurements and variables

The ultrasonic stadiometer (Shengyuan Co. Ltd, HGM-300, Henan, China) was used to measure the height (0.1 cm precision) and weight (0.1 kg precision). Body mass index (BMI) (kg/m^2) was calculated by the following equation: weight (kg)/$height^2$ (m^2). Obesity was defined as BMI higher than the 90th percentile for sex and age (21). Waist circumference (WC, cm) was collected at the end of expiration in children using an inelastic measuring tape. Child-specific validation blood pressure (BP)-measuring devices (Omron HEM-7012) was used

to measure BP by trained investigators. A portable ultrasound instrument (L12-4, CX30; Royal Philips, Amsterdam, The Netherlands) was used to measure the thickness of the left and right anterior and posterior walls at the proximal end of the common carotid sinus. cIMT value was calculated as the average of the sum of left anterior wall thickness, right anterior wall thickness, left posterior wall thickness, and right posterior wall thickness. Based on the reference value of cIMT for children aged 6 to 11 in China (22), high cIMT was defined as cIMT higher than the 90th percentile in each sex and age group.

For each participant, an automatic analyzer (Beckman Coulter, AU480, Mishima, Shizuoka, Japan) for triglyceride (TG), total cholesterol (TC), low-density lipoprotein cholesterol (LDL-C), and high-density lipoprotein cholesterol (HDL-C) were determined. Demographic information (such as age and gender) were collected through self-reported structured questionnaires.

Fecal collection and gut microbiome profiling

Fecal samples for all included children who had not received antibiotics within the past three months were collected and stored at -80°C. After gDNA was extracted and detected by 1% agarose gel electrophoresis, TransStart FastPfu DNA Polymerase (TransGen AP221-02) was used to amplify the V3–V4 region of 16S rDNA from gDNA. The primer sequences of the V3–V4 region were as follows: 338F (5'-ACTCCTACGGGAGGCAGCA-3') and 806R (5'-GGACTACHVGGGTWTCTAAT-3') (23). After quality control, detection, and quantification, TruSeqTM DNA Sample Prep Kit was used to construct the Miseq library, fix the generated single-stranded DNA fragments, and perform PCR synthesis and amplification, and then MiSeq Reagent Kit v3-600 cycles (Illumina, California, USA) on the Illumina MiSeq platform was used to sequence the library.

Bases with a quality value lower than 20 in the tail of Paired-end (PE) reads were filtered out to obtain the final optimized sequence. After removing single sequences without repetitions, non-repetitive sequences were extracted (http://drive5.com/usearch/manual/dereplication.html) and compared using the Silva database (Release138 http://www.arb-silva.de) (24). Operational taxonomic units (OTU) clustering was performed according to 97% similar non-repetitive sequences (25). After preprocessing, data were imported into Quantitative Insights into Microbial Ecology (QIIME version 1.9.1) for further analysis (26). The ribosomal database project classifier Bayesian algorithm was used to perform taxonomic analysis on the 97% similar level of OTU representative sequences (27), to obtain the species classification information corresponding to each OTU. The raw sequence reads have been stored in the NCBI Sequence Read Archive (PRJNA811365).

Statistical Analysis

Continuous variables with non-normal distribution were represented as Median (P25-P75), and categorical variables were represented as n (%). Non-parametric tests (Kruskal-Wallis H test) and Chi-square tests were used to compare continuous variables and categorical variables, respectively, among the normal group, OB + non-cIMT group, and OB + high-cIMT group. Two-sided P values < 0.05 indicate a significant difference.

Venn diagrams were used to visualize the number of overlap and unique OTUs in the three groups. A bar chart was used to show the species' composition. α-diversity analyses including Sobs, Shannon, Simpson, Ace, and Chao indicators were used to estimate the community richness and diversity of gut microbes, and the Wilcoxon rank-sum test was used to compare differences between every two groups. Benjamini-Hochberg was used to calculate P values adjusted for false discovery rate (FDR). The rarefaction curve was used to determine whether

the sequencing data are sufficient or not. In β-diversity analyses, principal coordinate analysis (PCoA) and nonmetric multidimensional scaling (NMDS) analysis were used to observe the difference in the composition of the overall gut microbiota between the three groups. The microbial biomarkers between each group were analyzed by linear discriminant analysis effect size (LEfSe). Significantly gut microbial markers were obtained using the non-parametric Kruskal-Wallis H test, and then linear discriminant analysis (LDA) to calculate the effect size of different microbiota (LDA $\geq$ 2.5). Random forest analysis was used to evaluate the degree of contribution of important biomarkers. The receiver operating characteristic (ROC) was used to evaluate the ability of biomarkers in identifying OB + non-cIMT group and OB + high-cIMT group from normal children. All analyses were performed using R version 3.3.1.

Phylogenetic Investigation of Communities by Reconstruction of Unobserved States (PICRUSt) analysis was used to standardize the OTU abundance table, and OTUs information based on the Greengene ID (28). The pathway information was obtained from the Kyoto Encyclopedia of Genes and Genomes (KEGG, http://www.genome.jp/kegg/) database, and the abundance of each pathway category was performed according to the OTU abundance. The predicted functional profiling of gut microbiota was presented using the extended error bar plot displayed in the STAMP version 2.1.3 with Welch's t-test for every two groups (29).

Results

Study population

A total of 72 children were included in this study including 24 children identified as OB + high-cIMT, 24 as OB + non-cIMT, and 24 as normal weight with normal cIMT matched by age and sex. The demographic and physical characteristics of the participants included in the study were presented in Table 1. The median age of included children was 10.79 years, of which 66.7% were boys. The BMI (16.55 vs. 23.77 vs. 26.18 kg/m^2), WC (60.63 vs. 81.85 vs. 85.85 cm), systolic blood pressure (SBP, 104.33 vs. 113.33 vs. 116.83 mmHg), and TG (0.81 vs. 1.15 vs. 1.18 mmol/L) were highest in the OB + high-cIMT group, followed by the OB + non-cIMT group and normal group. The HDL-C (1.83 vs. 1.43 vs. 1.39 mmol/L) was highest in the normal group, followed ty the OB + non-cIMT group and OB + high-cIMT group. There was no significant difference in age and sex distribution, TC, and LDL-C among these three groups.

Table 1
Characteristics of study participants.

	Overall (N = 72)	Normal (N = 24)	OB + non-cIMT (N = 24)	OB + high-cIMT (N = 24)	*P* value
Boys, %	48(66.7%)	16(66.7%)	16(66.7%)	16(66.7%)	NS
Age, years	10.8(10.5,11.1)	11.0(10.6,11.2)	10.7(10.5,11.0)	10.7(10.4,11.0)	NS
BMI, kg/m^2	23.8(17.5,25.8)	16.6(15.5,17.5)	23.8(23.0,24.8)	26.2(25.0,28.9)	<0.001
WC, cm	80.0(62.3,84.9)	60.6(57.5,62.7)	81.9(75.4,84.8)	85.9(83.0,91.9)	<0.001
SBP, mmHg	111.8(105.1,118.8)	104.3(100.8,109.8)	113.3(108.9,119.5)	116.8(111.8,123.7)	<0.001
TG, mmol/L	1.0(0.8,1.3)	0.8(0.6,0.9)	1.2(0.9,1.5)	1.2(1.0,1.6)	<0.001
TC, mmol/L	4.4(3.9,5.0)	4.2(3.8,4.8)	4.4(4.0,5.0)	4.5(4.0,5.3)	NS
LDL-C, mmol/L	2.4(2.0,3.0)	2.2(2.0,2.7)	2.6(2.0,3.0)	2.8(2.2,3.1)	NS
HDL-C, mmol/L	1.5(1.3,1.8)	1.8(1.5,2.0)	1.4(1.2,1.6)	1.4(1.2,1.6)	<0.001
GLU, mmol/L	5.0(4.7,5.4)	4.9(4.5,5.4)	5.0(4.8,5.4)	4.9(4.6,5.4)	NS

The median (P25-P75) and the percentage (%) were used to represent variables. OB + non-cIMT, obesity with normal carotid intima-media thickness; OB + high-cIMT, obesity with high carotid intima-media thickness; BMI, body mass index; WC, waist circumference; SBP, systolic blood pressure; TG, triglyceride; TC, total cholesterol; LDL-C, low-density lipoprotein cholesterol; GLU, glucose; HDL-C, high-density lipoprotein cholesterol; NS, not significant.

Gut microbial composition

A total of 3,909,618 optimization sequence number, 1,611,082,076 bases with an average length of 412.2 (min length: 208; max length: 529) was generated. A total of 642 OTUs were overlapped in these three groups, with 95 unique OTUs in the normal group, 68 unique OTUs in the OB + non-cIMT group, and 45 unique OTUs in the OB + high-cIMT group in the Venn diagram (Fig. 1A).

As shown in the bar chart, at the phylum level (Fig. 1B), *Firmicutes* was higher in the normal group (66.03%) than that in the OB + non-cIMT group (63.56%) and OB + high-cIMT group (63.89%), whereas *Bacteroidetes* was lower in the normal group (19.43%) compared with OB + non-cIMT group (21.63%) and OB + high-cIMT group (22.79%). Furthermore, the *Firmicutes/Bacteroidetes* (F/B) ratio was higher in the normal group (3.40) compared with the OB + non-cIMT group (2.94) and OB + high-cIMT group (2.80). At the genus level, *Faecalibacterium* (15.64% vs. 11.99% vs. 13.53%), *Bifidobacterium* (11.44% vs. 9.80% vs. 8.58%),

Subdoligranulum (8.33% vs. 5.94% vs. 5.06%) and *Blautia* (6.49% vs. 5.53% vs. 4.47%) were enriched in normal group, compared with OB + non-cIMT group and OB + high-cIMT group. *Bacteroides* (12.72% vs. 17.65% vs. 17.17%), *Agathobacter* (3.40% vs. 6.86% vs. 7.29%), and *Megamonas* (0.01% vs. 0.75% vs. 6.47%) were enriched in OB + high-cIMT group, compared to normal group and OB + non-cIMT group (Fig. 1C).

Gut microbial community diversity

α-diversity showed that the richness (Sobs, Ace, and Chao) in the OB + high-cIMT group was significantly lower than that in the normal group and OB + non-cIMT group (Fig. 2A-C), as well as the community diversity (Shannon and Simpson, Fig. 2D-E).

The flattened rarefaction curves of the gut microbes indicated that the sequencing depth was enough to represent the most microbial species (Sobs, Ace, Chao, Shannon, Simpson; Fig. 3A-E). PCoA analysis based on the Bray-Curtis distance algorithm showed that the microbial composition of OTU level in OB + high-cIMT group was significantly separated from the normal group and OB + non-cIMT group ($P < 0.01$, Fig. 4A). NMDS analysis similarly showed a significant difference between the composition of gut microbiota in these three groups ($R = 0.083$, $P < 0.01$, Fig. 4B).

Gut microbial biomarkers and potential value in risk assessment

At the phylum level, *Proteobacteria* was significantly enriched in the OB + high-cIMT group, followed by OB + non-cIMT and normal groups (Fig. 5A, $P_{FDR} < 0.05$). At the genus level, 14 significant genera were showed, such as *Alistipes*, *Christensenellaceae_R-7_group* (top 4 significant genera), and *unclassified_o__Bacteroidale* (top 4 significant genera) enriched in the normal group followed by OB + non-cIMT and OB + high-cIMT groups; *Intestinibacter*, *Ruminococcaceae_UCG-002*, *Family_XIII_AD3011_group* (top 4 significant genera), and *UBA1819* (top 4 significant genera) enriched in both normal and OB + non-cIMT groups, followed by OB + high-cIMT group; and *Lachnoclostridium* and *Lachnospiraceae_ND3007_group* enriched in the OB + high-cIMT group, follwed by OB + non-cIMT and normal groups (Fig. 5B, $P_{FDR} < 0.05$). OTU 408 in genus *Christensenellaceae_R-7_group*, OTU656 in genus *UBA1819*, OTU740 in genus *unclassified_o__Bacteroidales*, and OTU70 in genus *Family_XIII_AD3011_group* were significantly enriched in normal or both normal and OB + non-cIMT groups (Fig. 5C, $P_{FDR} < 0.05$). Based on the LDA score (Fig. 5D, LDA ≥ 2.5), LEfSe analysis (Fig. 5E) showed that at the genus level, *Alistipes* and *Christensenellaceae_R-7_group* were significantly enriched in the normal group, while *Lachnoclostridium* was significantly enriched in the OB + high-cIMT group.

Random forest analysis further showed that 2 of the top 4 significant genera, *Christensenellaceae_R-7_group* and *UBA1819* ranked as the two most important biomarkers (Fig. 6A). In addition, the other 2 of the top 4 significant genera, *unclassified_o__Bacteroidale* and *Family_XIII_AD3011_group* ranked in the top 6 and 12 in the random forest analysis, respectively. The ROC analysis showed that these four significant biomarkers had a high ability in discriminating OB + high-cIMT group from the normal group (area under the curve [AUC]: 0.91, 95% confidence interval [CI]: 0.82–1.00, Fig. 6B), and had moderate ability in distinguishing children with OB + non-cIMT from normal ones (AUC: 0.76, 95% CI: 0.62–0.91, Fig. 6C).

KEGG pathways contributing to the OB + high-cIMT children

We observed 5 significant KEGG pathways in normal group vs. OB + non-cIMT group ($P < 0.05$, Effect Size > 0.05, Fig. 7A). The thiamine metabolism and methane metabolism were increased in OB + non-cIMT group than in OB + high-cIMT group ($P < 0.05$, Effect Size > 0.01, Fig. 7B). There were 14 significant KEGG pathways between OB + high-cIMT group and normal group including the same 5 pathways in normal group vs. OB + non-cIMT group (Fig. 7A), most of which were linked to the hydrolysis of compounds and substrates ($P < 0.05$, Effect Size > 0.05, Fig. 7C).

Discussion

In this cross-sectional study, we identified dysbiosis of gut microbiota and microbial biomarkers correlated with the development and progress of obesity among children. The α-diversity of gut microbiota in OB + high-cIMT children and OB + non-cIMT children was decreased compared with the normal group. *Christensenellaceae_R-7_group*, *UBA1819*, *Family_XIII_AD3011_group*, and *unclassified_o__Bacteroidales* had moderate to high ability in discriminating OB + non-cIMT and OB + high-cIMT group from the normal group.

Emerging evidence among adults has shown that the dysbiosis of gut microbiota was associated with metabolic diseases such as obesity, diabetes, and cardiovascular diseases (30–32). Previous studies showed that the community diversity of gut microbiota was lower among children with type 1 diabetes or combined with other CVD risk factors, such as elevated blood pressure, compared with normal controls (33–35). However, the associations between gut microbiota and subclinical CVD among children have been less reported. To the best of our knowledge, we innovatively found that the overall gut microbial community diversity of gut microbiota was lower among children with OB + high-cIMT compared with OB + non-cIMT and normal controls. Our findings suggest that the high diversity of gut microbiota might be a preventive in the progress of obesity (i.e, OB + high-cIMT).

We identified that the relative abundance of phylum *Proteobacteria* and genus *Lachnoclostridium* was the highest among OB + high-cIMT children followed by those with OB + non-cIMT and normal ones, while *Alistipes* showed an opposite trend. Studies based on animals and adults similarly reported that the relative abundance of *Proteobacteria* was positively associated with obesity and its related metabolic disorder (36). Consistent with our results among children, *Alistipes* can be considered as an important protective biomarker for CVD and metabolic syndrome among Chinese adults (37, 38). In contrast, American studies among 54 subjects have suggested that *Alistipes* were associated with an increased BP (39). The discrepancy may be due to differences in sample size, age and sex distribution, ethnic groups, and different dietary patterns (40). Moreover, a large population-based cohort based on the TwinsUK registered adult twins showed that *Lachnoclostridium* was positively correlated with visceral fat and increased the risk of cardiometabolic diseases (41, 42). Our findings add to the existing evidence and suggest that *Proteobacteria*, *Alistipes*, and *Lachnoclostridium* might contribute to the development of obesity combined with cardiovascular damage among children.

We found that the relative abundance in genus *Christensenellaceae_R-7_group*, *UBA1819*, *Family_XIII_AD3011_group*, and *unclassified_o__Bacteroidales* were the top four significantly decreased genera in OB + high-cIMT children compared with normal groups. Our findings were supported by previous studies of related metabolic outcomes that increased relative abundance of *Christensenellaceae_R-7_group* had a protective effect on BP both in adults and mice (43, 44). Overrepresented *UBA1819* could improve the body weight in high-fat-fed mice and rats by reducing adipose tissue inflammation and glucolipid metabolism

disorder (45, 46). Although Shi et al. found the abundance of *Family_XIII_AD3011_group* was increased in high-fat-fed rats (46), a study reported by Lüll et al. among polycystic ovary syndrome women in Finland that *Family_XIII_AD3011_group* was decreased in females with obesity (47), and our findings among children were consistent with the latter. As reported by metagenomic sequencing on type 2 diabetes mice, the increased abundance of *unclassified_o__Bacteroidales* was associated with improved glycolipid metabolism (48). Interestingly, we firstly found that genus *Christensenellaceae_R-7_group*, *UBA1819*, *unclassified_o__Bacteroidales*, and *Family_XIII_AD3011_group* had moderate ability in identifying OB + non-cIMT from normal groups and high ability in identifying OB + high-cIMT from normal groups. Our findings suggest that a decreased abundance of genus *Christensenellaceae_R-7_group*, *UBA1819*, *Family_XIII_AD3011_group*, and *unclassified_o__Bacteroidales* play a vital role in the development of obesity and damage of carotid intima-media. Interventions targeting these biomarkers may be used as one of the non-invasive diagnoses of obese children with or without damage of carotid intima-media.

Moreover, we found that thiamine metabolism and methane metabolism were significantly lower in OB + high-cIMT group vs. OB + non-cIMT group. In addition, hydrolysis of compounds and substrates pathways contributed to differentiate OB + high-cIMT group from normal group. Thiamine was a cofactor for enzymes regulating glucose metabolism (49), and its concentrations were decreased in patients with type 1 and type 2 diabetes mellitus through the reinforcement of hyperglycemic damage (50). Several studies showed that the use of multivitamins that contained thiamine was inversely associated with myocardial infarction and may reduce the risk of CVD in adults (51, 52). Methane can be produced by *Methanomassiliicoccales*, which involves the progress of adult CVD (53), and plays a protective effect through anti-inflammation, anti-oxidation, and anti-apoptosis (54, 55). In addition, the imbalanced hydrolysis of compounds and substrates could affect intestinal permeability and microbiota density, which could lead to chronic inflammation (56–61). Our findings suggest that the development and progress of obesity might be mediated by gut microbiota through these pathways.

To the best of our knowledge, this is the first study to explore the association between gut microbiota and obesity with high cIMT in children, and we have found several biomarkers that have moderate to high ability in identifying OB + high-cIMT children and OB + non-cIMT children from normal children. However, several limitations should be noted. First, 16S rRNA sequencing generally does not provide a level of species resolution, and more comprehensive technologies, such as in vivo experiments in mice and metagenomic sequencing, are needed to analyze the underlying mechanisms of the gut microbiota in depth. Second, our case-control study cannot be used for causal inference. Third, our sample size is small compared with studies in adults which need to be further verified in large cohort studies. However, substantial changes in microbiota can be easily measured (62). The flattened rarefaction curves indicate that the sample size is sufficient and reasonable, and more samples will only produce a few new features. Fourth, our study is based on a single center, which needs to be validated in multiple centers and other ethnic groups.

In conclusion, we found that dysbiosis of gut microbiota is associated with obesity with or without carotid intima-media damage in children, and *Christensenellaceae_R-7_group*, *UBA1819*, *Family_XIII_AD3011_group*, and *unclassified_o_Bacteroidales* had the ability identifying obesity and its progress from normal status. Our study provides effective and targeted guidance for the interventions for children with obesity and target organ damage.

Declarations

Data availability

The raw sequence reads can be found under NCBI accession number PRJNA811365 and also available from the corresponding author Bo Xi (Email: xibo2007@126.com) upon request.

Acknowledgment

We are thankful to the National Natural Science Foundation of China for the funding support.

Author contributions

BX and JS designed the study. LY, XM, and MZ were involved in the data collection process, and JS performed data analysis. XJ wrote the first draft of the manuscript. SS was involved in language modification. All authors reviewed the manuscript and approved the final version for publication.

Conflict of interest

The authors declare that they have no conflicts of interest.

Ethical approval

The study protocol was approved by the Institutional Ethics Review Board of the School of Public Health, Shandong University.

Funding

This work was supported by the National Natural Science Foundation of China (Grant ID: 81722039, 81673195), China Postdoctoral Science Foundation (Grant ID: 2021M701978), Natural Science Foundation of Shandong (Grant ID: ZR2021QH272).

References

1. Blüher M. Obesity: global epidemiology and pathogenesis. Nature reviews Endocrinology. 2019;15(5):288–98.
2. Zhao D, Liu J, Wang M, Zhang X, Zhou M. Epidemiology of cardiovascular disease in China: current features and implications. Nature reviews Cardiology. 2019;16(4):203–12.
3. Tedstone A, Duval D, Peacock E. Dietary health and CVD: implications for dietary policy in England. Proc Nutr Soc. 2020;79(1):95–102.

4. Greenland P, Alpert JS, Beller GA, Benjamin EJ, Budoff MJ, Fayad ZA, et al. 2010 ACCF/AHA guideline for assessment of cardiovascular risk in asymptomatic adults: a report of the American College of Cardiology Foundation/American Heart Association Task Force on Practice Guidelines. J Am Coll Cardiol. 2010;56(25):e50-103.
5. Willeit P, Tschiderer L, Allara E, Reuber K, Seekircher L, Gao L, et al. Carotid Intima-Media Thickness Progression as Surrogate Marker for Cardiovascular Risk: Meta-Analysis of 119 Clinical Trials Involving 100 667 Patients. Circulation. 2020;142(7):621–42.
6. Romero-Corral A, Montori VM, Somers VK, Korinek J, Thomas RJ, Allison TG, et al. Association of bodyweight with total mortality and with cardiovascular events in coronary artery disease: a systematic review of cohort studies. Lancet. 2006;368(9536):666–78.
7. van Mil SR, Biter LU, van de Geijn GJM, Birnie E, Dunkelgrun M, Ijzermans JNM, et al. The effect of sex and menopause on carotid intima-media thickness and pulse wave velocity in morbid obesity. Eur J Clin Invest. 2019;49(7):e13118.
8. Rychter AM, Naskręt D, Zawada A, Ratajczak AE, Dobrowolska A, Krela-Kaźmierczak I. What Can We Change in Diet and Behaviour in Order to Decrease Carotid Intima-Media Thickness in Patients with Obesity? Journal of personalized medicine. 2021;11(6):505.
9. Zucchini S, Fabi M, Maltoni G, Zioutas M, Trevisani V, Di Natale V, et al. Adolescents with severe obesity show a higher cardiovascular (CV) risk than those with type 1 diabetes: a study with skin advanced glycation end products and intima media thickness evaluation. Acta Diabetol. 2020;57(11):1297–305.
10. Ma CW, Yang L, Zhao M, Xi B. Association of abdominal obesity and obesity types with carotid intima-media thickness in children in China. Chinese Journal of Epidemiology. 2020;41(9):1450–4.
11. Witkowski M, Weeks TL, Hazen SL. Gut Microbiota and Cardiovascular Disease. Circul Res. 2020;127(4):553–70.
12. Tang WH, Kitai T, Hazen SL. Gut Microbiota in Cardiovascular Health and Disease. Circul Res. 2017;120(7):1183–96.
13. He M, Shi B. Gut microbiota as a potential target of metabolic syndrome: the role of probiotics and prebiotics. Cell & bioscience. 2017;7:54.
14. Sommer F, Bäckhed F. The gut microbiota–masters of host development and physiology. #N/A. 2013;11(4):227–38.
15. Ussar S, Griffin NW, Bezy O, Fujisaka S, Vienberg S, Softic S, et al. Interactions between Gut Microbiota, Host Genetics and Diet Modulate the Predisposition to Obesity and Metabolic Syndrome. Cell Metab. 2015;22(3):516–30.
16. Sang T, Guo C, Guo D, Wu J, Wang Y, Wang Y, et al. Suppression of obesity and inflammation by polysaccharide from sporoderm-broken spore of Ganoderma lucidum via gut microbiota regulation. Carbohydr Polym. 2021;256:117594.
17. Perry RJ, Peng L, Barry NA, Cline GW, Zhang D, Cardone RL, et al. Acetate mediates a microbiome-brain-β-cell axis to promote metabolic syndrome. Nature. 2016;534(7606):213–7.
18. Zhang C, Yin A, Li H, Wang R, Wu G, Shen J, et al. Dietary Modulation of Gut Microbiota Contributes to Alleviation of Both Genetic and Simple Obesity in Children. EBioMedicine. 2015;2(8):968–84.

19. Hou YP, He QQ, Ouyang HM, Peng HS, Wang Q, Li J, et al. Human Gut Microbiota Associated with Obesity in Chinese Children and Adolescents. Biomed Res Int. 2017;2017:7585989.
20. Yang LL, Zhang Q, Zhang YQ, Sun JH, Zhao M, Xi B. Design of Huantai Childhood Cardiovascular Health Cohort Study. Chinese Journal of Epidemiology. 2020;54(12):1461–4.
21. Li H, Zong XN, Ji CY, Mi J. Body mass index cut-offs for overweight and obesity in Chinese children and adolescents aged 2–18 years. Zhonghua liu xing bing xue za zhi = Zhonghua liuxingbingxue zazhi. 2010;31(6):616–20.
22. Yang L, Zong XN, Liu Q, Hou YP, Zhao M, Xi B. The preliminary development of reference values of carotid artery intima-media thickness in children aged 6–11 years. Chinese Journal of Epidemiology. 2019;53(7):696–700.
23. Claesson MJ, O'Sullivan O, Wang Q, Nikkilä J, Marchesi JR, Smidt H, et al. Comparative analysis of pyrosequencing and a phylogenetic microarray for exploring microbial community structures in the human distal intestine. PLoS One. 2009;4(8):e6669.
24. Quast C, Pruesse E, Yilmaz P, Gerken J, Schweer T, Yarza P, et al. The SILVA ribosomal RNA gene database project: improved data processing and web-based tools. Nucleic Acids Res. 2013;41(Database issue):D590-6.
25. Edgar RC. Search and clustering orders of magnitude faster than BLAST. Bioinformatics. 2010;26(19):2460–1.
26. Bolyen E, Rideout JR, Dillon MR, Bokulich NA, Abnet CC, Al-Ghalith GA, et al. Reproducible, interactive, scalable and extensible microbiome data science using QIIME 2. Nat Biotechnol. 2019;37(8):852–7.
27. Cole JR, Wang Q, Cardenas E, Fish J, Chai B, Farris RJ, et al. The Ribosomal Database Project: improved alignments and new tools for rRNA analysis. Nucleic Acids Res. 2009;37(Database issue):D141-5.
28. Douglas GM, Maffei VJ, Zaneveld JR, Yurgel SN, Brown JR, Taylor CM, et al. PICRUSt2 for prediction of metagenome functions. Nat Biotechnol. 2020;38(6):685–8.
29. Parks DH, Tyson GW, Hugenholtz P, Beiko RG. STAMP: statistical analysis of taxonomic and functional profiles. Bioinformatics. 2014;30(21):3123–4.
30. Ma J, Li H. The Role of Gut Microbiota in Atherosclerosis and Hypertension. Front Pharmacol. 2018;9:1082.
31. Lau K, Srivatsav V, Rizwan A, Nashed A, Liu R, Shen R, et al. Bridging the Gap between Gut Microbial Dysbiosis and Cardiovascular Diseases. #N/A. 2017;9(8):859.
32. Weiss GA, Hennet T. Mechanisms and consequences of intestinal dysbiosis. Cellular and molecular life sciences: CMLS. 2017;74(16):2959–77.
33. Lakshmanan AP, Shatat IF, Zaidan S, Jacob S, Bangarusamy DK, Al-Abduljabbar S, et al. Bifidobacterium reduction is associated with high blood pressure in children with type 1 diabetes mellitus. Biomedicine & pharmacotherapy = Biomedecine & pharmacotherapie. 2021;140:111736.
34. Leiva-Gea I, Sánchez-Alcoholado L, Martín-Tejedor B, Castellano-Castillo D, Moreno-Indias I, Urda-Cardona A, et al. Gut Microbiota Differs in Composition and Functionality Between Children With Type 1 Diabetes and MODY2 and Healthy Control Subjects: A Case-Control Study. Diabetes Care. 2018;41(11):2385–95.
35. Del Chierico F, Manco M, Gardini S, Guarrasi V, Russo A, Bianchi M, et al. Fecal microbiota signatures of insulin resistance, inflammation, and metabolic syndrome in youth with obesity: a pilot study. Acta Diabetol. 2021;58(8):1009–22.

36. Machate DJ, Figueiredo PS, Marcelino G, Guimarães RCA, Hiane PA, Bogo D, et al. Fatty Acid Diets: Regulation of Gut Microbiota Composition and Obesity and Its Related Metabolic Dysbiosis. Int J Mol Sci. 2020;21(11).
37. Jie Z, Xia H, Zhong SL, Feng Q, Li S, Liang S, et al. The gut microbiome in atherosclerotic cardiovascular disease. Nat Commun. 2017;8(1):845.
38. Qin Q, Yan S, Yang Y, Chen J, Li T, Gao X, et al. A Metagenome-Wide Association Study of the Gut Microbiome and Metabolic Syndrome. Front Microbiol. 2021;12:682721.
39. Stevens BR, Pepine CJ, Richards EM, Kim S, Raizada MK. Depressive hypertension: A proposed human endotype of brain/gut microbiome dysbiosis. Am Heart J. 2021;239:27–37.
40. Wu GD, Chen J, Hoffmann C, Bittinger K, Chen YY, Keilbaugh SA, et al. Linking long-term dietary patterns with gut microbial enterotypes. Science. 2011;334(6052):105–8.
41. Nogal A, Louca P, Zhang X, Wells PM, Steves CJ, Spector TD, et al. Circulating Levels of the Short-Chain Fatty Acid Acetate Mediate the Effect of the Gut Microbiome on Visceral Fat. Front Microbiol. 2021;12:711359.
42. Wang G, Zhang Y, Zhang R, Pan J, Qi D, Wang J, et al. The protective effects of walnut green husk polysaccharide on liver injury, vascular endothelial dysfunction and disorder of gut microbiota in high fructose-induced mice. Int J Biol Macromol. 2020;162:92–106.
43. Calderón-Pérez L, Llauradó E, Companys J, Pla-Pagà L, Pedret A, Rubió L, et al. Interplay between dietary phenolic compound intake and the human gut microbiome in hypertension: A cross-sectional study. Food Chem. 2021;344:128567.
44. Liu Y, Li T, Alim A, Ren D, Zhao Y, Yang X. Regulatory Effects of Stachyose on Colonic and Hepatic Inflammation, Gut Microbiota Dysbiosis, and Peripheral CD4(+) T Cell Distribution Abnormality in High-Fat Diet-Fed Mice. J Agric Food Chem. 2019;67(42):11665–74.
45. Hu Q, Niu Y, Yang Y, Mao Q, Lu Y, Ran H, et al. Polydextrose Alleviates Adipose Tissue Inflammation and Modulates the Gut Microbiota in High-Fat Diet-Fed Mice. Front Pharmacol. 2021;12:795483.
46. Shi J, Zhao D, Song S, Zhang M, Zamaratskaia G, Xu X, et al. High-Meat-Protein High-Fat Diet Induced Dysbiosis of Gut Microbiota and Tryptophan Metabolism in Wistar Rats. J Agric Food Chem. 2020;68(23):6333–46.
47. Lüll K, Arffman RK, Sola-Leyva A, Molina NM, Aasmets O, Herzig KH, et al. The Gut Microbiome in Polycystic Ovary Syndrome and Its Association with Metabolic Traits. The Journal of clinical endocrinology and metabolism. 2021;106(3):858–71.
48. Wang R, Zhang L, Zhang Q, Zhang J, Liu S, Li C, et al. Glycolipid Metabolism and Metagenomic Analysis of the Therapeutic Effect of a Phenolics-Rich Extract from Noni Fruit on Type 2 Diabetic Mice. J Agric Food Chem. 2022;70(9):2876–88.
49. Volvert ML, Seyen S, Piette M, Evrard B, Gangolf M, Plumier JC, et al. Benfotiamine, a synthetic S-acyl thiamine derivative, has different mechanisms of action and a different pharmacological profile than lipid-soluble thiamine disulfide derivatives. BMC pharmacology. 2008;8:10.
50. Frank J, Kisters K, Stirban OA, Obeid R, Lorkowski S, Wallert M, et al. The role of biofactors in the prevention and treatment of age-related diseases. BioFactors. 2021;47(4):522–50.

51. Rautiainen S, Akesson A, Levitan EB, Morgenstern R, Mittleman MA, Wolk A. Multivitamin use and the risk of myocardial infarction: a population-based cohort of Swedish women. Am J Clin Nutr. 2010;92(5):1251–6.
52. Howe CG, Li Z, Zens MS, Palys T, Chen Y, Channon JY, et al. Dietary B Vitamin Intake Is Associated with Lower Urinary Monomethyl Arsenic and Oxidative Stress Marker 15-F(2t)-Isoprostane among New Hampshire Adults. J Nutr. 2017;147(12):2289–96.
53. Fadhlaoui K, Arnal ME, Martineau M, Camponova P, Ollivier B, O'Toole PW, et al. Archaea, specific genetic traits, and development of improved bacterial live biotherapeutic products: another face of next-generation probiotics. Appl Microbiol Biotechnol. 2020;104(11):4705–16.
54. Boros M, Ghyczy M, Érces D, Varga G, Tőkés T, Kupai K, et al. The anti-inflammatory effects of methane. Crit Care Med. 2012;40(4):1269–78.
55. Ye ZH, Ning K, Ander BP, Sun XJ. Therapeutic effect of methane and its mechanism in disease treatment. Journal of Zhejiang University Science B. 2020;21(8):593–602.
56. Llewellyn SR, Britton GJ, Contijoch EJ, Vennaro OH, Mortha A, Colombel JF, et al. Interactions Between Diet and the Intestinal Microbiota Alter Intestinal Permeability and Colitis Severity in Mice. Gastroenterology. 2018;154(4):1037-46.e2.
57. Moore KJ, Sheedy FJ, Fisher EA. Macrophages in atherosclerosis: a dynamic balance. #N/A. 2013;13(10):709–21.
58. Zou Y, Yang Y, Fu X, He X, Liu M, Zong T, et al. The regulatory roles of aminoacyl-tRNA synthetase in cardiovascular disease. Molecular therapy Nucleic acids. 2021;25:372–87.
59. Grajeda-Iglesias C, Aviram M. Specific Amino Acids Affect Cardiovascular Diseases and Atherogenesis via Protection against Macrophage Foam Cell Formation: Review Article. Rambam Maimonides medical journal. 2018;9(3).
60. Delarue M. Aminoacyl-tRNA synthetases. Curr Opin Struct Biol. 1995;5(1):48–55.
61. Oprescu SN, Griffin LB, Beg AA, Antonellis A. Predicting the pathogenicity of aminoacyl-tRNA synthetase mutations. Methods. 2017;113:139–51.
62. Dunn WB, Broadhurst D, Begley P, Zelena E, Francis-McIntyre S, Anderson N, et al. Procedures for large-scale metabolic profiling of serum and plasma using gas chromatography and liquid chromatography coupled to mass spectrometry. Nat Protoc. 2011;6(7):1060–83.

Figures

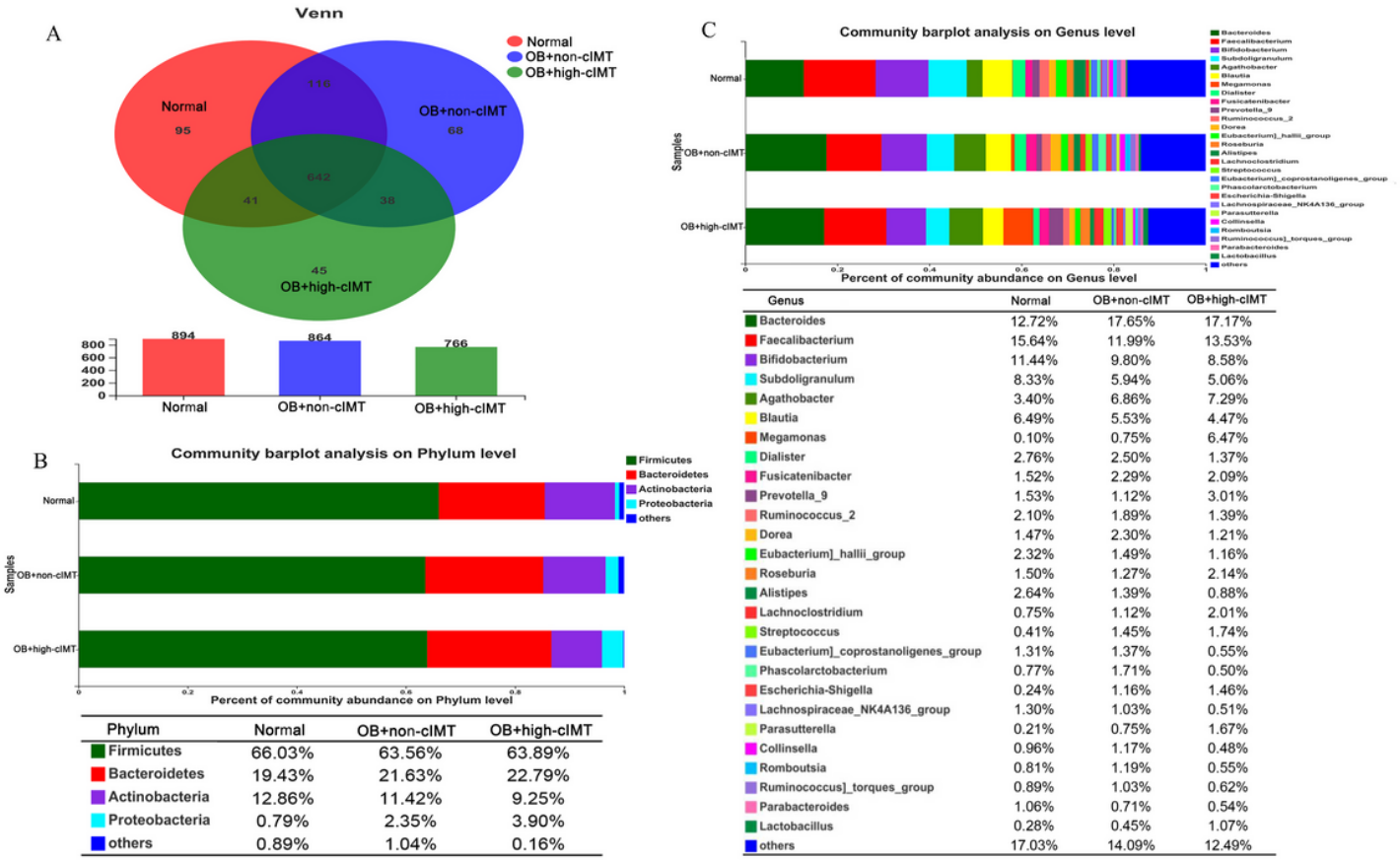

Phylum	Normal	OB+non-cIMT	OB+high-cIMT
Firmicutes	66.03%	63.56%	63.89%
Bacteroidetes	19.43%	21.63%	22.79%
Actinobacteria	12.86%	11.42%	9.25%
Proteobacteria	0.79%	2.35%	3.90%
others	0.89%	1.04%	0.16%

Genus	Normal	OB+non-cIMT	OB+high-cIMT
Bacteroides	12.72%	17.65%	17.17%
Faecalibacterium	15.64%	11.99%	13.53%
Bifidobacterium	11.44%	9.80%	8.58%
Subdoligranulum	8.33%	5.94%	5.06%
Agathobacter	3.40%	6.86%	7.29%
Blautia	6.49%	5.53%	4.47%
Megamonas	0.10%	0.75%	6.47%
Dialister	2.76%	2.50%	1.37%
Fusicatenibacter	1.52%	2.29%	2.09%
Prevotella_9	1.53%	1.12%	3.01%
Ruminococcus_2	2.10%	1.89%	1.39%
Dorea	1.47%	2.30%	1.21%
Eubacterium]_hallii_group	2.32%	1.49%	1.16%
Roseburia	1.50%	1.27%	2.14%
Alistipes	2.64%	1.39%	0.88%
Lachnoclostridium	0.75%	1.12%	2.01%
Streptococcus	0.41%	1.45%	1.74%
Eubacterium]_coprostanoligenes_group	1.31%	1.37%	0.55%
Phascolarctobacterium	0.77%	1.71%	0.50%
Escherichia-Shigella	0.24%	1.16%	1.46%
Lachnospiraceae_NK4A136_group	1.30%	1.03%	0.51%
Parasutterella	0.21%	0.75%	1.67%
Collinsella	0.96%	1.17%	0.48%
Romboutsia	0.81%	1.19%	0.55%
Ruminococcus]_torques_group	0.89%	1.03%	0.62%
Parabacteroides	1.06%	0.71%	0.54%
Lactobacillus	0.28%	0.45%	1.07%
others	17.03%	14.09%	12.49%

Figure 1

Gut microbial taxonomic composition in the normal, OB+non-cIMT, and OB+high-cIMT groups. **(A)** The Venn diagram showed the shared OTUs in the three groups. The Bar diagram showed gut microbial composition at the **(B)** phylum level, and **(C)** genus level in the three groups, respectively.

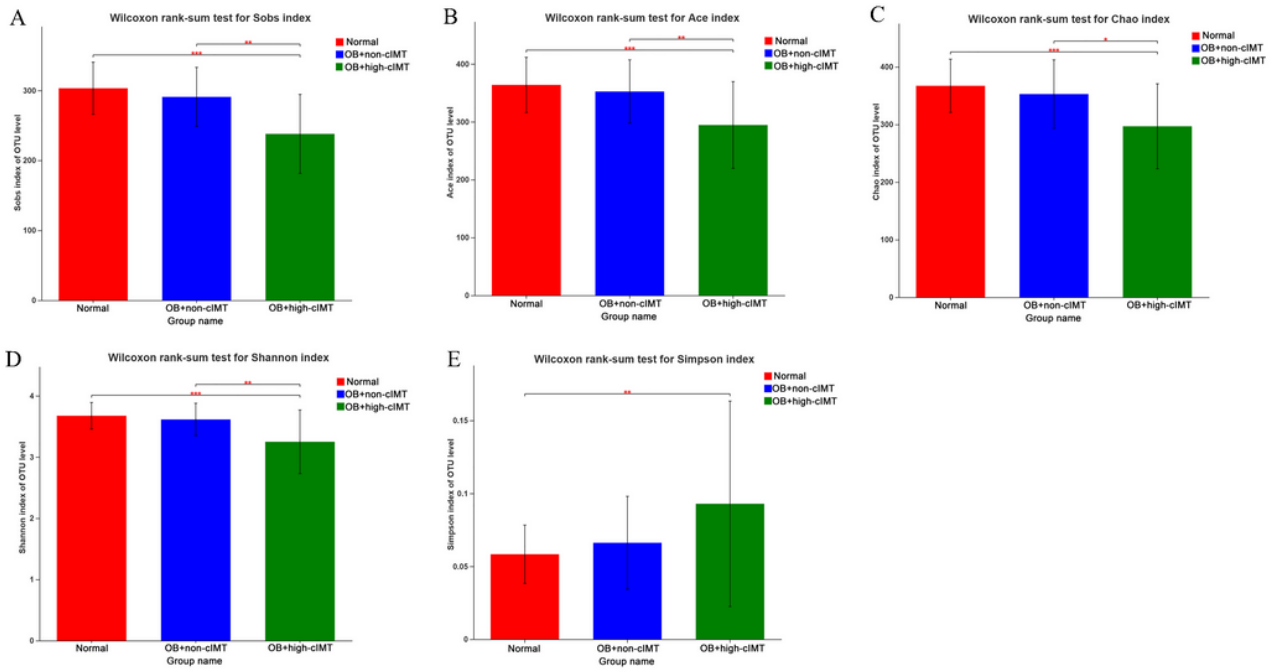

Figure 2

α-diversity was measured by **(A)** Sobs, **(B)** Ace, **(C)** Chao, **(D)** Shannon and **(E)** Simpson indexes. (* $P < 0.05$, ** $P < 0.01$, *** $P < 0.001$)

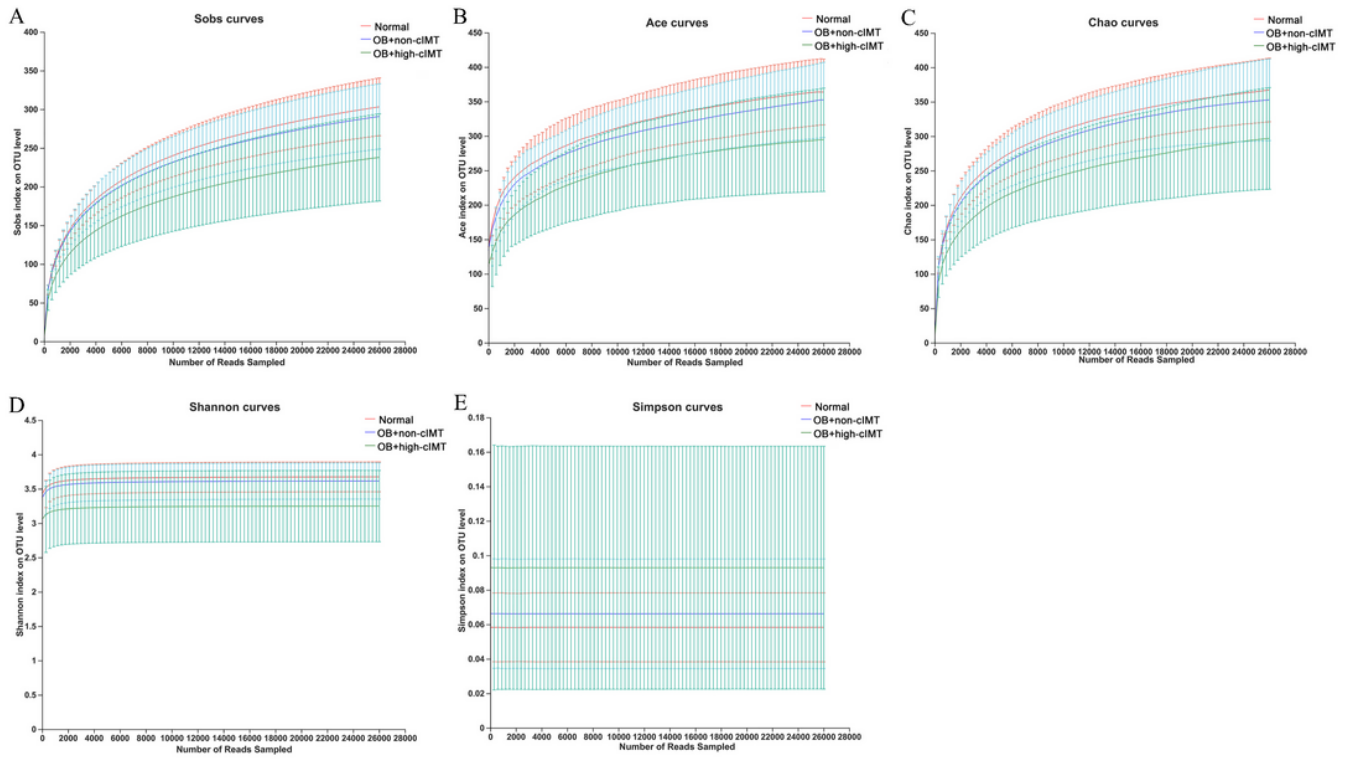

Figure 3

Calculate the rarefaction curves of each sample at OTU level, **(A)** for Sobs, **(B)** for Ace, **(C)** for Chao, **(D)** for Shannon, and **(E)** for Simpson. Average of the samples in the group.

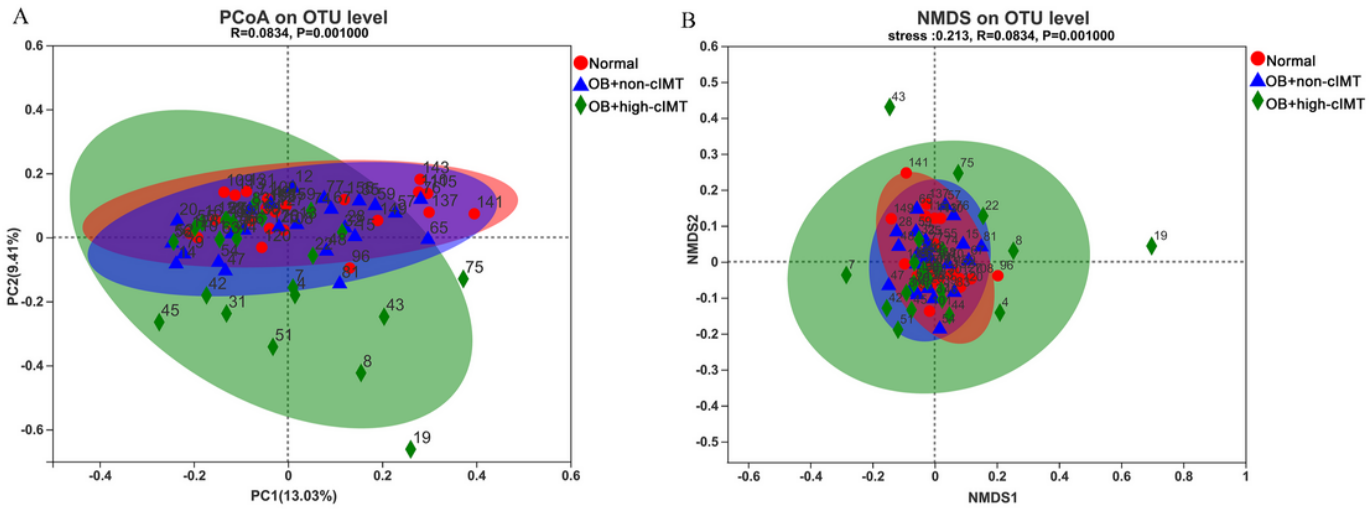

Figure 4

β-diversity was calculated by the Bray-Curtis distance algorithm using **(A)** principal coordinate analysis (PCoA, PC1=13.03%, PC2=9.41%) and **(B)** nonmetric multidimensional scaling (NMDS) based on the relative abundance profile of OTUs.

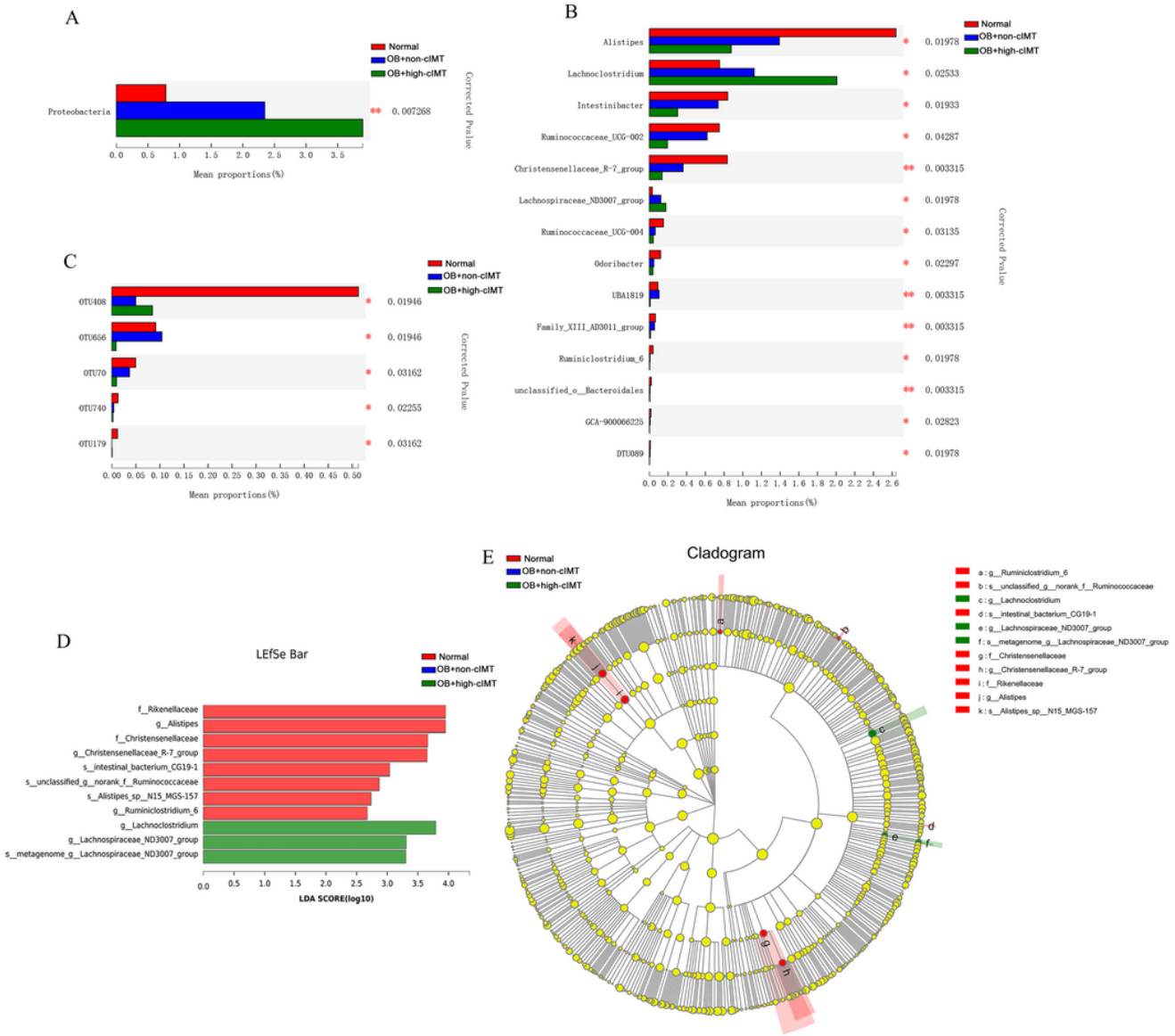

Figure 5

The non-parametric Kruskal-Wallis H test revealed gut microbial markers of **(A)** species, **(B)** genus, and **(C)** OTU levels. **(D)** Linear discriminant analysis (LDA, LDA ≥ 2.5) score of each microbial biomarker. **(E)** Cladogram showed the main bacterial biomarkers from phylum to species. The larger the diameter of each circle, the greater the relative abundance of the taxa. (p, phylum; c, class; o, order; f, family; g, genus; s, species; Unclassified as a mark without classification information; * $P < 0.05$, ** $P < 0.01$)

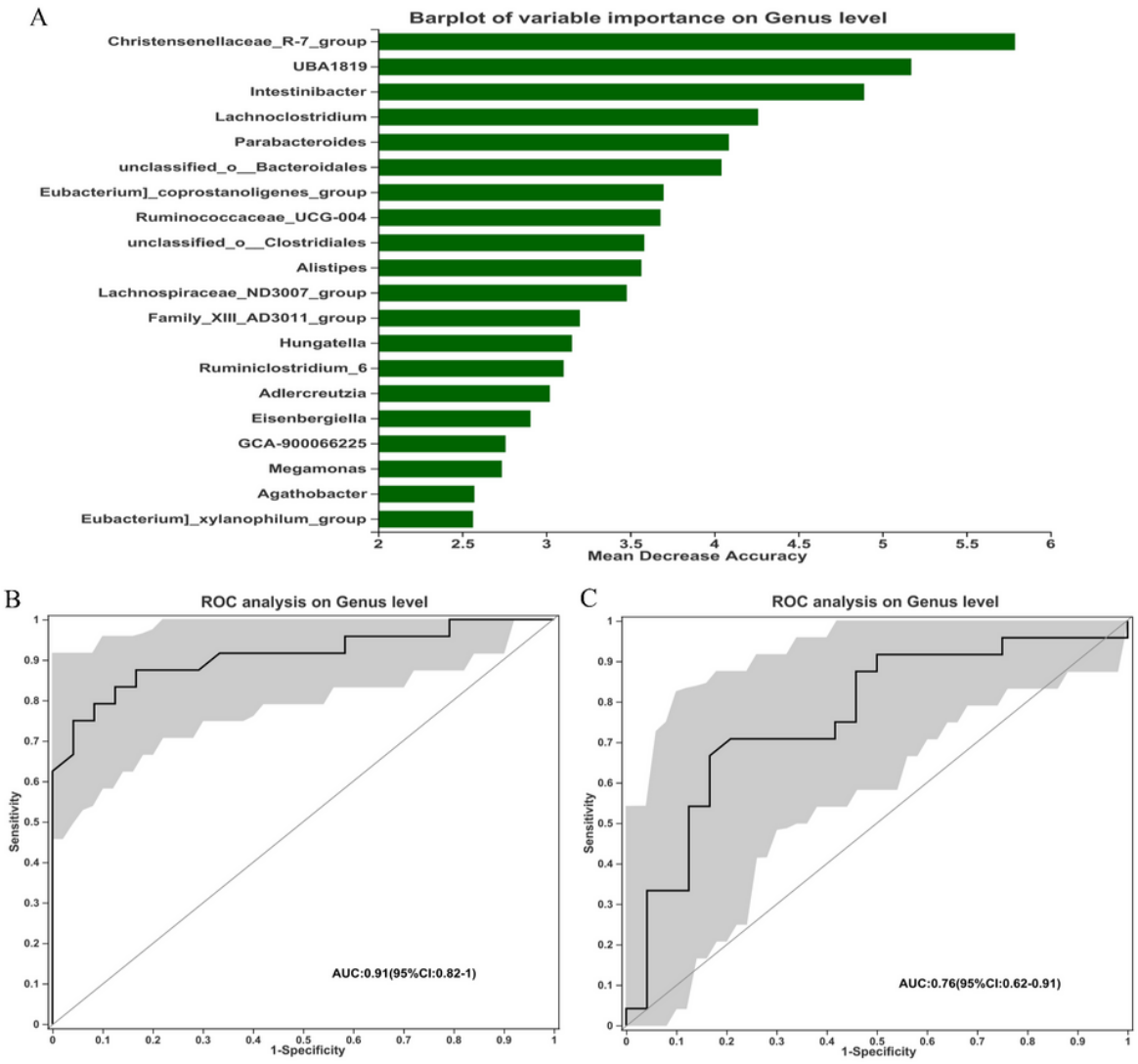

Figure 6

(A) Random Forest Model showed the relative abundance ranking of genera. **(B)** ROC analysis assesses the ability of the biomarker genera to identify OB+high-cIMT vs. normal, and the gray area under the curve (AUC, 0.91) represents the 95% confidence interval (CI, 0.82-1.00). **(C)** ROC analysis assesses the ability of the biomarker genera to identify OB+non-cIMT vs. normal, and the AUC was 0.76 (95% CI, 0.62-0.91).

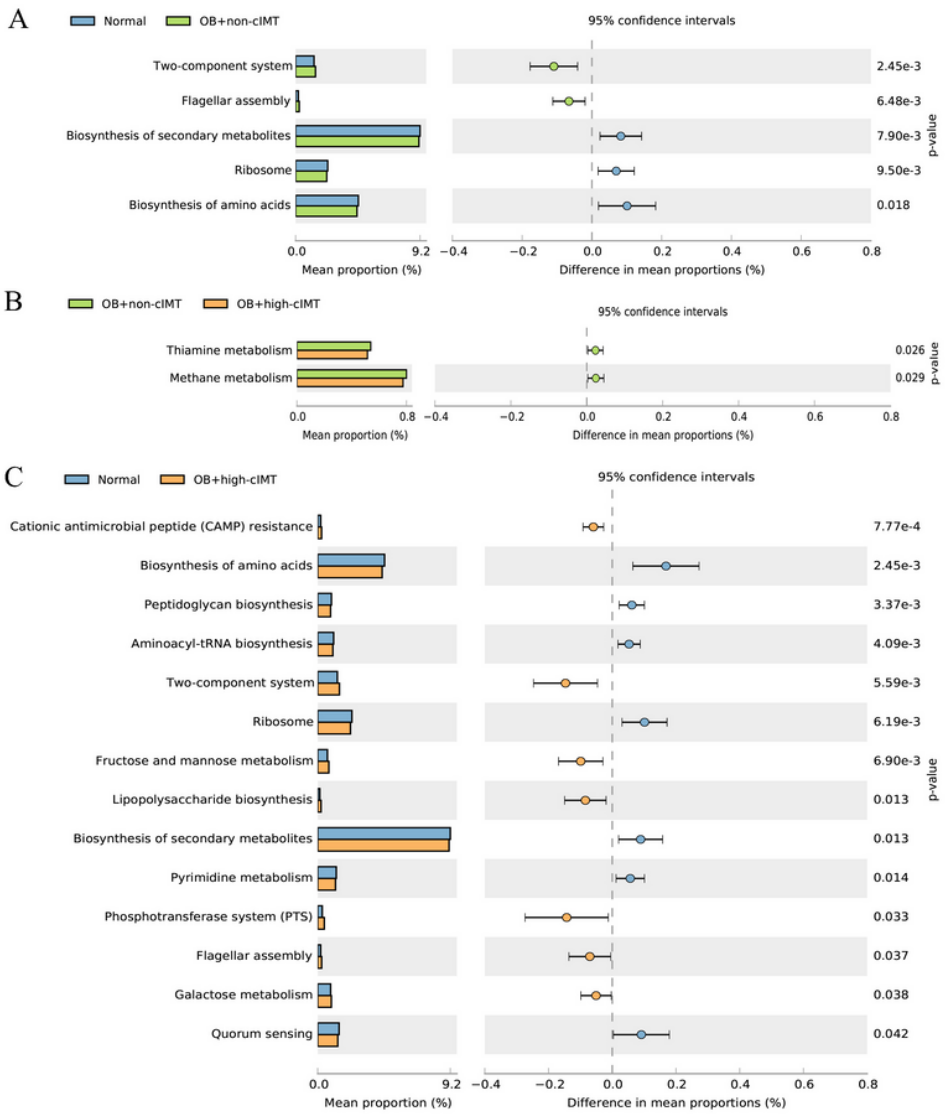

Figure 7

(A-C) Extended error bars plot shows the KEGG functional pathways predicted by PICRUSt in each two groups between the normal, OB+non-cIMT, and OB+high-cIMT groups. ($P < 0.05$)